Regulatory Properties of Tropomyosin Effects of Length, Isoform, and N-Terminal Sequence†

R. Maytum,*,‡ M. Konrad,§ S. S. Lehrer,|| and M. A. Geeves‡,||

Department of Biosciences, University of Kent at Canterbury, Canterbury, U.K., Max-Planck-Institut für Biophysikalische Chemie, Am Fassberg 11, D-37070 Göttingen, Germany, and Muscle Research Group, Boston Biomedical Research Institute, 64 Grove Street, Watertown, Massachusetts 02472

Received January 10, 2001; Revised Manuscript Received April 11, 2001

ABSTRACT: The regulatory properties of naturally occurring tropomyosins (Tms) of differing lengths have been examined. These Tms span from 4 to 7 actin subunits. Native proteins have been used to study the common 7 actin-spanning skeletal and smooth muscle variants and expressed recombinant proteins to study the shorter fibroblast 5a, 5b, yeast Tm1 and yeast Tm2 Tms (6, 6, 5, and 4 actin-spanning variants, respectively). The yTm2 has been overexpressed in *Escherichia coli* with N-terminal constructs equivalent to those previously used for yTm1 [Maytum, R., et al. (2000) *Biochemistry 39*, 11913]. The regulation of myosin subfragment 1 (S1) binding to actin by Tm has been assessed using a sensitive S1 binding titration. The equilibrium between closed and open (C to M states, $K_T = 0.1-0.14$) was similar for all vertebrate Tms. Apart from skTm where the apparent cooperative unit size (n) is the same as the structural size ($n = 7$ actin sites), the other vertebrate Tms that were studied exhibited large n values ($n = 12-14$). The yeast Tms also exhibited large values of n (6−9) in comparison to their structural sizes (4−5). The determined value of K_T depended on the N-terminal sequence ($K_T = 0.15-1$). These results are compared with the effect of S1 upon Tm's affinity for actin. The yeast Tms have regulatory parameters similar to those of skTm, but unlike skTm, S1 has little effect upon their actin affinity. This shows that an actin state with a high affinity for S1 and Tm is not necessary for regulation, and the higher affinity of S1 for actin in the presence of vertebrate Tms is probably the result of a direct interaction of S1 with Tm.

Tropomyosin (Tm)[1] is an actin-binding, α-helical coiled-coil molecule which appears to be ubiquitous among eukaryotic cells, having been identified in organisms ranging from yeast (*Saccharomycetes cerevisiae*) to humans. It consists of parallel homo- or heterodimers (of equivalent isoforms from different genes) of two fully α-helical chains of identical length, although the length can vary according to isoform type. These isoforms result from different genes as well as from alternatively spliced RNA transcripts. Higher organisms produce around 20 Tm isoforms from up to four separate genes (*1*, *2*). All these isoforms are either approximately 284 or 248 amino acids in size and overlap 7 or 6 actins. Shorter Tm isoforms, spanning only 5 or 4 actin subunits, have been identified in *S. cerevisiae* having 2 single exon genes (*TPM1* and *TPM2*) expressing proteins of 199 (yTm1) or 161 (yTm2) amino acids (*3*, *4*).

The best understood role of Tm is in skeletal and cardiac muscle where in combination with the calcium-dependent troponin (Tn) regulatory complex it regulates the binding of myosin to actin and hence muscle contraction. The role of Tm in non-muscle tissue is less clear. In vivo studies have shown differential localization of Tm isoforms across developing neurons and some other cultured cell types. Differential expression has also been found during cell transformation and differentiation. This suggests that different isoforms are required for specific roles in regulating both the actin filament structure and the interaction of other proteins with the actin cytoskeleton (*2*).

The binding of myosin to actin becomes cooperative in the presence of Tm, indicating that there are at least two regulatory states which switch between states in groups of more than one actin subunit. Troponin confers calcium sensitivity upon the system, producing a modulation of regulation in response to calcium concentration (*5*, *6*). As shown in Figure 1, the regulatory system has been shown to have three states that can be biochemically differentiated (*7*) which were termed blocked, closed, and open and appear to be related to three different positions found for Tm on actin (*8*). To clarify the structural and biochemical properties of these states, it has recently been suggested that these should be termed the B (blocked, no myosin binding), C (calcium-induced, "closed"), and M (myosin-induced, "open") states (*9*). In the skeletal system in the presence of Tn and the absence of calcium, the B (70%) and C (30%) states are mainly occupied and Tm appears to be localized upon the outer domain of actin. In the presence of calcium or when

† R.M. and M.A.G. were supported by Welcome Trust Grant 055841. M.K. was supported by the Max Planck Institute. S.S.L. and M.A.G. were supported by NIH Grants HL22461 and AR 41637.

* To whom correspondence should be addressed. Telephone: +44 1227 823950. Fax: +44 1227 763912. E-mail: rmm@ukc.ac.uk.

‡ University of Kent at Canterbury.

§ Max-Planck-Institut für Biophysikalische Chemie.

|| Boston Biomedical Research Institute.

[1] Abbreviations: Tm, tropomyosin; S1, myosin subfragment 1; yTm, yeast tropomyosin; skTm, skeletal tropomyosin; smTm, smooth muscle tropomyosin; PCR, polymerase chain reaction; Tn, troponin; MOPS, 4-morpholinepropanesulfonic acid.

10.1021/bi010072i CCC: $20.00
Published on Web 05/24/2001

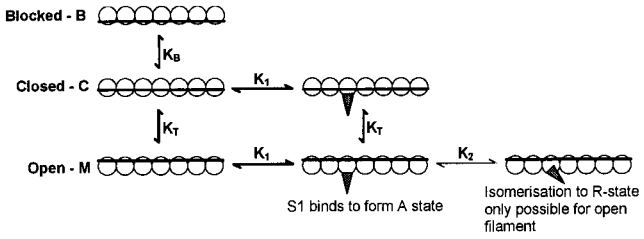

FIGURE 1: Three-state model of the thin filament as proposed by McKillop and Geeves (*7*). The A_7−Tm−Tn structural unit is shown as seven open circles representing the actins connected via a line representing the tropomyosin. This unit exists in a dynamic equilibrium between the three states as represented by the different positions of tropomyosin. The three states are the blocked state in which no S1 binding can occur, the closed state in which only weak binding can occur, and the open state which allows isomerization of the S1 to the rigor-like state. The ratio of the three states in the absence of S1 is defined by the equilibrium constants K_B (between the blocked and closed states) and K_T (between the closed and open states). The blocked state is only present in the absence of Ca^{2+} when the Tn complex is tightly bound to the filament, in the presence of Tn and Ca^{2+}, or when Tn is absent, there is little or no occupancy of the blocked state, meaning K_B is large and can be ignored.

Tm alone is present, the C state (80%) and some M state (20%) are occupied and Tm is localized upon the inner domain near the junction of the two domains. The M state, where Tm is localized on the inner domain, is exclusively present only with myosin bound (*9*).

The structural repeat unit of the skeletal muscle actin−tropomyosin−troponin complex of A_7TmTn has been used as the cooperative unit size in most models of thin filament regulation (*7*, *10*). It is now becoming accepted that the apparent cooperative unit size is not dependent upon the structural unit size. The basis for this is the idea that the end-to-end interaction of Tm produces a continuous filament along the actin backbone, and it is then the flexibility of this filament which governs the apparent cooperative unit size rather than the structural unit (*11*, *12*). Evidence for this enhanced cooperativity was first shown for fluorescently labeled skTm in the presence of Tn (*13*) or fragments of TnT (*14*) and later for both smooth muscle (smTm) and fibroblast Tm 5a (*11*). We have recently used a sensitive fluorescence titration technique using phalloidin-stabilized pyrene-labeled actin to characterize the binding of S1 to actin in the skeletal system (*12*). Binding curves are of sufficient accuracy to allow fitting to a version of the three-state model allowing for a variable apparent cooperative unit size (n) and allowing K_T (the equilibrium between the closed and open states) to be determined explicitly for the first time. The results showed that as expected in the presence of Tn and calcium the apparent cooperative unit size was considerably greater (11−12) than the structural unit size (7). We have also applied this technique to a set of N-terminal mutants of yTm1 which showed significantly different S1 binding to actin that was dependent upon the N-terminal sequence. The data all showed greater cooperativity (n = 8−9) compared to their structural unit size (5), and the differences between the curves could be accounted for purely by changes in K_T (0.14−1).

We have now extended our studies of Tm properties using this technique to cover examples from all of the different lengths of naturally occurring Tms, spanning from 4 to 7 actin units. To facilitate this, we have expressed yTm2 in *Escherichia coli* for the first time, producing a set of N-terminal constructs (necessary for actin binding) equivalent to those previously produced for yTm1 (*15*). We have also expressed recombinant fibroblast Tms 5a and 5b as examples of 6 actin subunit-spanning vertebrate non-muscle isoforms. These have been previously shown to be expressed well in *E. coli* and bind to actin without N-terminal acetylation, which does not take place in *E. coli* (*16*). In contrast, skeletal Tm requires N-terminal acetylation to bind to actin (*17*, *18*). We have therefore used purified native skeletal (rabbit muscle) and smooth (chicken gizzard) Tms as examples of 7 actin-spanning Tms.

In this work, these Tms are characterized using both titration and cosedimentation techniques. We contrast measurements of their affinity for actin and for the skeletal and yeast Tms with measurements of their affinity for actin saturated with S1, with the regulatory parameters determined by fitting of their S1 binding curves. The implications of these results upon the regulatory mechanism are discussed.

MATERIALS AND METHODS

DNA Constructs. General recombinant DNA techniques were performed as described by Sambrook et al. (*19*) or as recommended by the supplier.

The yeast *TPM1(n2)* construct in pJC20 was produced as described previously (*15*).

Yeast *TPM2* was cloned from total yeast genomic DNA by standard PCR using Taq polymerase (Roche Molecular Biochemicals) with primers designed to match the N- and C-terminal coding regions and including *Nde*I and *Bam*HI (*italic*) subcloning sites, respectively, for insertion into the pJC20 expression vector (*20*). The sequences used for the primers were as follows: 5′-GGAATTC*CAT ATG* GAG AAG ATC AAA GAG AAA TTG-3′ (5′-forward primer) and 5′-CGC*GGATCC*T CAT AAA TTT TCC AAT GAA TTA GC-3′ (3′-reverse primer). The 0.5 kb PCR product was cut with *Nde*I and *Bam*HI, ligated into pJC20, and transformed into *E. coli* strain XL-1 Blue. *TPM2* mutants were produced by PCR using combinations of the 3′-reverse *TPM2* primer along with 5′-primers, including the modified sequences (underlined) for the 5′-terminus (see Figure 2). The 5′ primers were designed as for the original primer to include the *Nde*I site for cloning into the expression vector. The sequences for the primers that were used were as follows: TPM2(*n*2), 5′-GGAATTC*CAT ATG* GCG AGC ATG GAG AAG ATC AAA GAG-3′; TPM2(*n*5), 5′-GGAATTC*CAT ATG* GCG GGT AGC AGC TCT ATG GAG AAG ATC AAA GAG-3′; and TPM2(*n*9), 5′-GGAATTC*CAT ATG* GCG GGT AGC AGC TCG CTG GAG GCG GTG AAA GAG AAA TTG AAT AGC-3′.

Clones of rat fibroblast tropomyosins 5a and 5b were amplified from PET8c (gift from M. Gimona and D. Helfman) using PCR primers designed to introduce *Nde*I and *Bam*HI restriction sites for cloning into pJC20. The sequences for the primers that were used were as follows: TPM5a and -5b, 5′-GGAATTC*CAT ATG* GCG GGT AGC AGC TCG CTG GCG-3′ (5′-forward primer) and 5′-CGC*GGATCC*T CAC ATG TTG TTT AGC TCC AGT AAA G-3′ (3′-reverse primer). Identical primers were used for both TPM5a and TPM5b as they differ only by an internal alternatively spliced exon (see Figure 2). As for the *TPM2* clones, the ligated

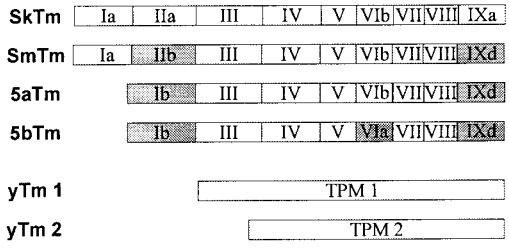

sk/smTm	**MDAIKKKMQM**
5a/b	**(M)** AGSSSLEAVRR**K**IRS
yTm 1	**MD**KIRE**K**LSN
yTm 2	**M**EKI**KE**K**L**NS
yTm2 (n_2)	**(M)** AS**MEKIKEKLNS**
yTm2 (n_5)	**(M)** AGSSS**MEKIKEKLNS**
yTm2 (n_9)	**(M)** AGSSSLEAV**KEKLNS**

FIGURE 2: Sizes and exon structures of the 4 vertebrate and 2 yeast Tm genes used in this work. From the top, skeletal and smooth muscle isoforms which contain 284 amino acid residues spanning 7 actin subunits and differing in the second and ninth exons are shown. Below are the fibroblast 5a and 5b isoforms containing 247 amino acids which span 6 actin subunits. These have a smooth muscle-like C-terminus with the first two exons replaced with a single alternative exon 1b. They differ internally by the alternative exon 6a/6b. At the bottom are the two shorter 5- and 4-actin-spanning (199 and 161 amino acids, respectively) yeast isoforms which are both encoded as a single exon. Below are sequence comparisons of the different N-termini of the vertebrate and yeast Tms showing the 5-amino acid residue extension present in alternative exon 1b. At the bottom are N-terminal constructs of yTm2 made on the basis of either the dipeptide extension or the exon 1b sequence. For both the fibroblast and yeast Tms, the N-terminal Met is removed post-translationally and is therefore shown in brackets. Since these isoforms are expressed in *E. coli*, they also lack the native N-terminal acetylation.

plasmids were transformed into *E. coli* XL-1 Blue for plasmid replication.

The entire coding regions of the constructs were verified by automatic DNA sequencing (Applied Biosystems 373 sequencer) using a dye-based PCR sequencing reaction.

Protein Expression and Purification. For expression, all the clones were transformed in the BL-21 DE3(pLys) cells and expressed and purified as previously described (*15*). In brief, 1 L cultures were grown to late-exponential phase and induced for 3 h with 0.4 mM IPTG. Cells were harvested, resuspended in 60 mL of lysis buffer [20 mM Tris (pH 7.5), 100 mM NaCl, 2 mM EDTA, 1 mg/L DNAse, and 1 mg/L RNAse], and lysed by passing them through a French press (15 000 psi). The majority of *E. coli* proteins were precipitated by heating to 80 °C for 10 min, and the precipitated protein and cell debris were removed by centrifugation. The soluble Tm was then isoelectrically precipitated at pH 4.5 using 0.3 M HCl. The precipitate was pelleted and resuspended in 10−20 mL (dependent upon yield) of running buffer [10 mM phosphate (pH 7.0) and 100 mM NaCl]. This was then further purified using a 6 mL Pharmacia Resource-Q column, eluted with a 150 to 400 mM NaCl gradient, the Tm eluting at ∼200−250 mM salt as found previously for recombinant yTm1. Fractions were analyzed by SDS−PAGE, pooled, and concentrated by isoelectric precipitation. Extinction coefficients for recombinant proteins were calculated from the sequences using AnTheProt (G. Deleage, IBCP-CNRS). Yeast Tm protein concentrations were estimated using extinction coefficients $E^{1\%}$ at 280 nm of 8.2 and 6.0 cm^{-1} for yTm2 and yTm1, respectively, and fibroblast 5a and 5b concentrations using an extinction coefficient of 1.6 cm^{-1}.

Electrospray Mass Spectrometry. Protein molecular masses were determined by electrospray mass spectrometry. Small (50 μL) stock samples were dialyzed overnight against 1 mM Tris (pH 7.0), acidified with formic acid, and applied to a Finnegan Mat LCQ ion-trap MS system fitted with a nanospray device. Mass accuracy for Tm samples is expected to be 2−4 Da (1/10000). Predicted molecular masses for proteins were calculated using AnTheProt with Delta Mass (ABRF) used to determine mass differences due to modifications.

Other Proteins and Reagents. Myosin subfragment 1 (S1) was prepared by chymotryptic digestion of rabbit myosin, as described by Weeds and Taylor (*21*). Its molar concentration was calculated from the absorbance measurement at 280 nm using an $E^{1\%}$ of 7.9 cm^{-1} and a molecular mass of 115 000 Da. Rabbit actin was purified by the method of Spudich and Watt (*22*). Its molar concentration was determined by its absorbance at 280 nm using an $E^{1\%}$ of 11.08 cm^{-1} and a molecular mass of 40 000 Da. The preparation of pyrene-labeled actin (pyr-actin) was as previously described (*23*). Phalloidin (Boehringer)-stabilized F-actin was made by incubating a solution of 10 μM pyrene-labeled actin with 10 μM phalloidin overnight in experimental buffer [20 mM MOPS (pH 7.0), 200 mM KCl, and 5 mM $MgCl_2$] at 4 °C.

Chicken gizzard tropomyosin (smTm) and rabbit skeletal Tm (skTm) were purified by isoelectric precipitation and ammonium sulfate fractionation as previously described (*6*, *24*).

Fluorescence Titrations. Fluorescence titrations were carried out at 20 °C using either an SLM 8100 spectrofluorimeter with excitation at 365 nm with an 8 nm bandwidth and emission at 405 nm with a 16 nm bandwidth or a Perkin-Elmer 50B spectrofluorimeter at the same wavelengths using 10 nm excitation and 15 nm emission slits. A total working volume of 2 mL was used in a 10 mm × 10 mm cell constantly being stirred using a magnetic stirrer below the light path of the instrument. Autotitrations were carried out by the continuous addition of a concentrated S1 stock solution into a continuously stirred cell using a Harvard Apparatus Syringe Infusion Pump 22 driving a 100 μL glass syringe (Hamilton) as described previously (*12*). Data were acquired over a period of 250 s, with data points being collected every 0.5 s, using an integration time of 0.45 s. Buffer solutions for the titrations were filtered using a 0.22 μm disposable syringe filter to remove dust particles which can produce significant noise in the stirred cell at the low levels of sample fluorescence that were used. The use of a 10 mm × 10 mm cell (2 mL volume) reduces the effects of dilution (only 50 μL in total is added during a titration) and fluorescence bleaching (only a small fraction of the continuously mixed solution is exposed to the light source at any time). Mixing and equilibration of the reaction in the cell were checked as described in detail previously (*12*).

Cosedimentation and Quantitative Electrophoresis. Cosedimentation assays were performed by mixing actin with

binding proteins (Tm and myosin) at relevant concentrations in the standard assay buffer [20 mM MOPS (pH 7.0), 200 mM KCl, and 5 mM $MgCl_2$] to a total volume of 200 μL. The actin was then pelleted (along with any bound proteins) by centrifugation at 100000*g* for 20 min (Beckmann model TL100A). Equivalent samples of the pellet and supernatant were then separated by SDS−polyacrylamide gel electrophoresis (SDS−PAGE). SDS−PAGE was performed according to the method of Laemmli (*25*) using 13.5% acrylamide gels and stained with Coomassie Blue G-250. Quantification of proteins was carried out by using a Umax Powerlook III scanner with a transparency adapter attached to a personal computer. The scanner was calibrated using a Kodak neutral density step tablet, and scanned images were analyzed using the Image-PC program (Scion Corp.; based upon NIH-Image).

MODELING

Binding can be monitored by the quenching of a pyrene label attached to actin. The fraction of actin bound is then directly proportional to the change in fluorescence.

$$\alpha = \frac{F_0 - F}{F_0 - F_\infty} \quad (1)$$

In a system containing only tropomyosin, the blocked state of the three-state model (*7*) is assumed to be absent. A simpler two-state version (discarding the $1/K_B$ term) of the three-state equation from Maytum et al. (*12*) for a cooperative unit size *n* can therefore be used as shown previously (*15*). K_1 (binding to the A state), K_2 (A to R isomerization), and K_T (the closed−open equilibrium) are as shown previously (*12*).

$$\alpha = \frac{K_1[\mathrm{M}]P^{n-1}[K_T(1+K_2)^n + 1]}{(K_T P^n + Q^n + 1/K_B)(1+K_2)^{n-1}} \quad (2)$$

where α is as defined in eq 1, [M] is in this case the concentration of free S1, $P = 1 + K_1[M](1 + K_2)$ and $Q = 1 + K_1[\mathrm{M}]$.

Fitting of the binding curves was achieved by a process of systematic variation of *n* and examination of the sum of the residuals and specific deviations for each value as described in detail previously (*12*).

RESULTS

Expression of Recombinant Proteins. The TPM2 constructs were successfully expressed in *E. coli*, giving yields of ~30 mg/L, noticeably higher than for the similar TPM1 constructs previously expressed (*15*). The purified proteins [yTm2(*nX*)] ran on SDS−PAGE at the anomalous molecular mass of 26 kDa as previously shown for the native protein overexpressed in yeast (*4*). All the expressed constructs bound to actin with half-saturation, $K_{50\%}$, in the 0.5 μM range as seen previously for the yTm1 constructs [only yTm1(*n*2) data shown; see Figure 3]. For all these constructs, it was expected that the N-terminal Met would be removed by post-translational processing as seen for the yTm1 constructs (*15*) to leave Ala as the first amino acid. Mass spectrometry of the recombinant proteins gave molecular masses of 19 254.6, 19 487.0, and 19 427.8 Da compared to predicted masses for the unmodified proteins lacking the N-terminal Met of 19 252, 19 483.3, and 19 426 Da, respectively. This indicated that all the proteins were of the expected mass lacking the N-terminal Met and showing no other post-translational processing such as acteylation or phosphorylation.

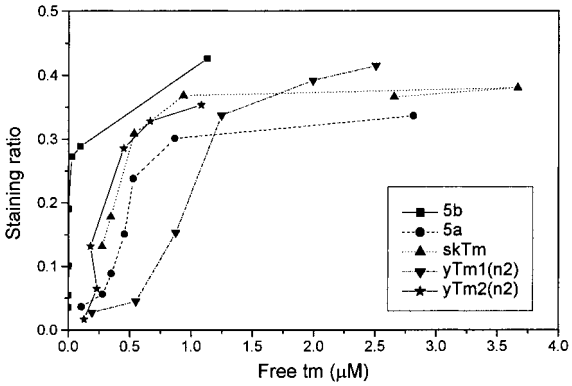

FIGURE 3: Curves for binding of the differing Tms (as denoted by the legend) to actin determined by cosedimentation. Varying concentrations of tropomyosin were mixed with 10 μM actin in 20 mM MOPS (pH 7.0), 200 mM KCl, and 5 mM $MgCl_2$ and then cosedimented at 100000*g* for 20 min. Equivalent samples of the supernatant and pellet were separated by SDS−PAGE, and the concentrations of free and bound tropomyosin were determined by quantitative scanning of the Coomassie blue-stained gels. The *y*-axis is plotted as the ratio of the absorbance of the Tm/actin bands in the pellet.

Fibroblast Tms 5a and 5b were expressed at levels lower than those seen for the yeast proteins, yielding 10−20 mg/L. The two clones have identical N-terminal sequences, and as for the yeast sequences, it was expected that the N-terminal Met would be removed post-translationally to leave Ala as the first amino acid. No evidence was seen of a significant nonbinding fraction of expressed protein as shown previously by Pittinger and Helfman for 5a (*26*).

Mass spectrometry of the expressed proteins shows masses of 28 425.2 and 28 566.2 Da, corresponding to predicted masses of 28 426.7 and 28 566.0 Da for the proteins lacking their N-terminal Met and with no other modification, respectively.

Affinity of Tropomyosin for Actin. The affinities of the various tropomyosins for actin, determined by cosedimentation, are shown in Figure 3. It can be seen that all the affinities ($K_{50\%}$ which indicates half-saturation of Tm binding to actin) fall in the range of 0.2−0.8 μM except for that of 5b which is just too tight to measure accurately in our system as it appears to be close to the detection limit of ~0.05 μM. Previous work has shown 5b's affinity to be ~2 μM (*26*) in a Mg^{2+} free buffer and its binding approximately 10-fold tighter than that of 5a under similar conditions (*27*).

Effect of Myosin S1 upon Tm Binding to Actin. The effect of saturating concentrations of S1 upon binding of yTm1-(*n*2) to actin is shown in Figure 4. It can be clearly seen that the presence of bound S1 produces a slight decrease in the affinity of yTm1(*n*2) for actin. This is in contrast to the effect of S1 upon the binding of vertebrate Tms to actin where it increases their affinity by 1000−10000-fold (*28*, *29*). A comparison of the affinities of skTm and yTm1(*n*2) is shown in Figure 5. In the absence of S1, skTm and yTm1(*n*2) have similar affinities for actin (0.4 and 0.8 μM, respectively). However, in the presence of S1, there is no detectable free skTm until saturation of the filament is reached (affinity ≪

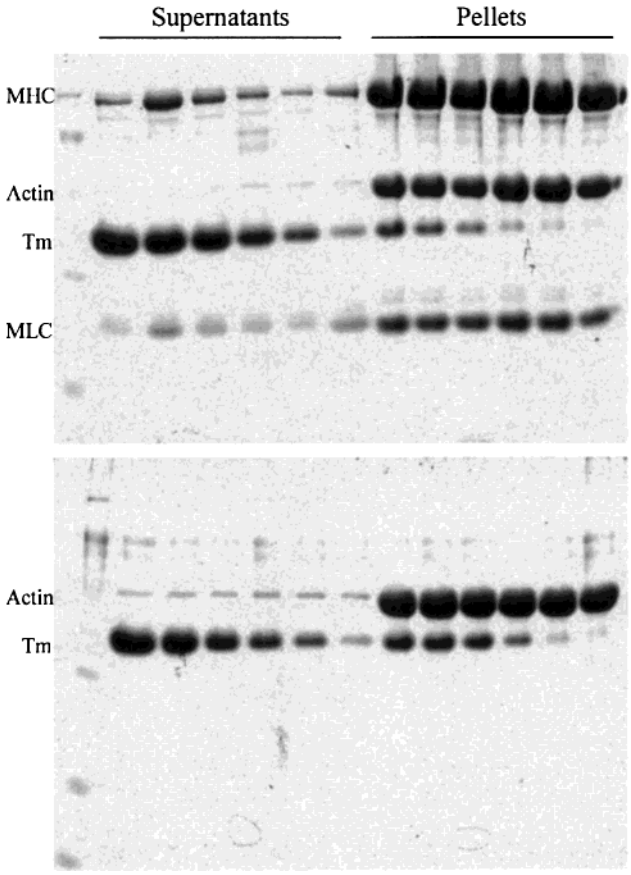

FIGURE 4: Comparison of the binding of yTm1(*n*2) to actin in the absence (bottom) and presence (top) of myosin S1. Buffer conditions as described in the legend of Figure 3 with 10 μM actin mixed with (from right to left in each gel, with supernatants and pellets as marked) 0.2, 0.5, 1, 2, 3, and 4 μM Tm with or without 11 μM myosin S1. The myosin heavy and light chains are clearly separated from the actin and Tm. Comparison of the two gels shows that the presence of S1 has little effect upon the affinity of yTm1(*n*2) for actin.

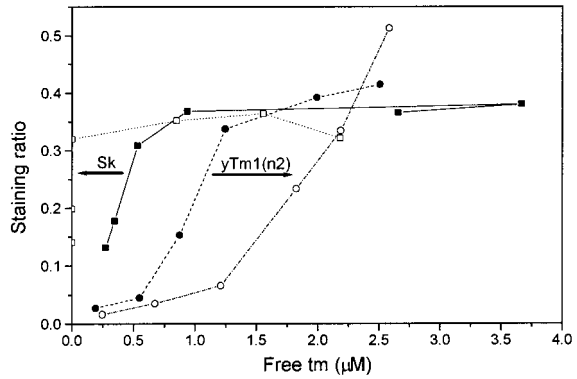

FIGURE 5: Comparison of the effect of S1 upon the binding of yTm1(*n*2) and skTm to actin assessed as described in the legend of Figure 3. Curves are shown with filled symbols for Tm alone and with open symbols with S1 present. In the presence of saturating concentrations of S1, the level of binding of skTm is greatly increased and the binding too tight to assess under these conditions, while in stark contrast, the affinity of yTm1(*n*2) appears to be little changed by the presence of S1.

0.05 μM), while the affinity of yTm1(*n*2) is similar to that in the absence of S1, showing a dramatic difference between the two. For the other yeast Tm construct, yTm2(*n*2), the binding constant in the presence of S1 was difficult to quantify exactly as on SDS−PAGE the myosin light chains

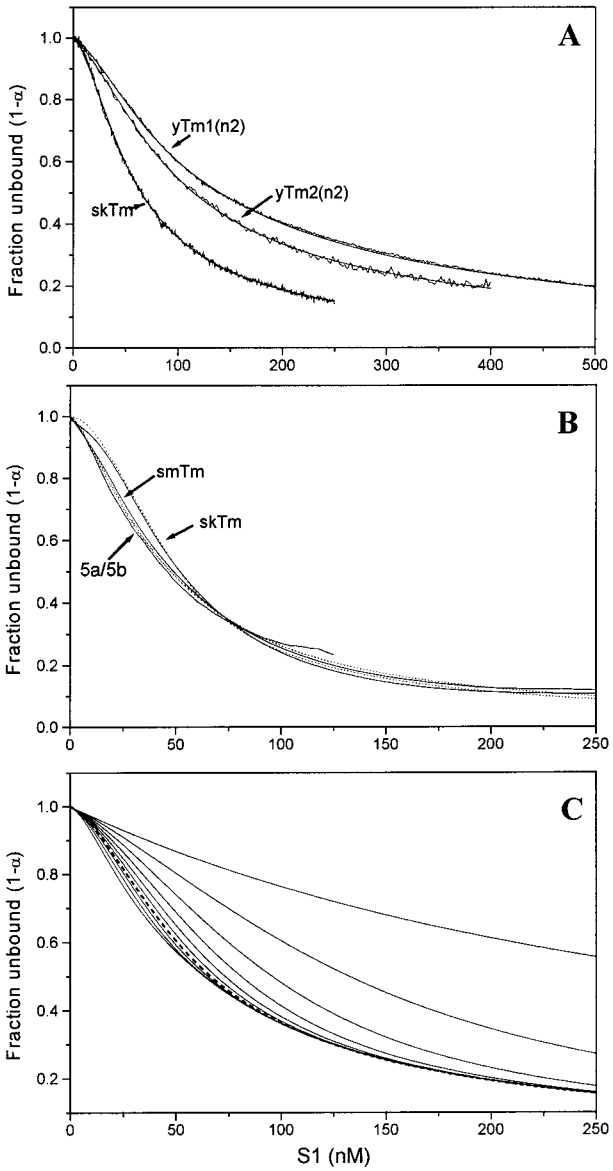

FIGURE 6: Curves for myosin S1 binding to 50 nM phalloidin-stabilized pyrene-labeled actin, in 20 mM MOPS (pH 7.0), 200 mM KCl, and 5 mM $MgCl_2$. (A) Actin with 2 μM yTm1(*n*2), yTm2(*n*2), and skTm showing the similar shapes (K_T and *n*) but differing affinities (K_1K_2) for the three Tms. (B) Actin with 2 μM skTm, smTm, and Tms 5a and 5b. Only one curve is shown for 5a and 5b as their titration curves were identical. For both panels A and B, the data are shown superimposed with fitted curves to the cooperative binding model (eq 2) with the values listed in Table 1. (C) Simulated curves showing the effect of varying *n* from 1 to 14 (from top to bottom; $n = 7$ is shown as the dotted line), with the other parameters set as for skTm.

and yTm2 have similar motilities (data not shown). However, by comparison of the supernatant concentrations of Tm and the staining of the combined Tm/LC bands, it could be clearly seen that yTm1(*n*2) also showed little change in affinity for actin in the presence of S1.

S1 Binding to Actin−Tm Complexes. Equilibrium titrations of myosin S1 to actin were carried out under the same conditions as used previously for both the skeletal system (*12*) and yeast Tm1 (*15*). All titrations contained Tm at 2 μM, significantly above the determined $K_{50\%}$ for all the Tms to ensure saturation of the filaments with Tm.

Figure 6 shows comparative titration data for the two yeast

Table 1: Parameters for Curve Fits to Tms

	skTm	smTm	5a/5b	yTm1(*n*2)	yTm2(*n*2)
K_1 ($\times 10^4$ M^{-1})	13	12	12	4.43	4.22
K_2	200	200	200	200	200
K_T	0.14	0.1	0.1	0.37	0.33
n	7	12	14	9	7

Table 2: Parameters for Curve Fits to yTm2 Mutants (equivalent yTm1 in brackets)

	yTm2(*n*2)	yTm2(*n*5)	yTm2(*n*9)
K_1 ($\times 10^4$ M^{-1})	4.2 [4.4]	4.4 [2.8]	4.8 [3.8]
K_2	200	200	200
K_T	0.33 [0.37]	0.44 [1]	0.16 [0.14]
n	7 [9]	6 [8]	6 [8]

Tms, yTm1(*n*2) and yTm2(*n*2), and the archetypal vertebrate Tm, skTm. All three data sets are shown with fitted curves superimposed with the parameters for the curve fits shown in Table 1. For the curve fitting, the value of K_2 is defined as the previously determined value of 200 as this is a property of actin and myosin (*30*). Comparison of the curves shows that the affinities of S1 for the actin filaments containing the two yeast Tms are both similar to each other and differ little from the affinity of S1 for actin alone [as shown previously for yTm1 (*15*)]. This clearly differs from the S1 affinity for filaments containing skTm, for which the S1 affinity is approximately 3-fold higher. This is reflected by the K_1 values determined for the curve fits which are similar for yTm1(*n*2) and yTm2(*n*2) (4.43×10^4 and 4.22×10^4 M^{-1}, respectively) and ~3-fold lower than that for skTm (12×10^4 M^{-1}). Both the yTms exhibit similar values for K_T (0.37 and 0.33, respectively) and a slight difference in the apparent cooperative unit size (9 and 7, respectively) which is approximately twice the size of the structural repeat (5 and 4, respectively) in both cases. Although shifted to the left by the higher S1 affinity, the shape of the curve for skTm is very similar to that for the yTms with a similar determined value for the apparent cooperative unit size (7) and a K_T (0.14) which differs by a factor of only 2.

Figure 6B shows titration curves for the vertebrate Tms, the two muscle isoforms, skTm and smTm, and the two fibroblast isoforms, 5a and 5b. The exon composition of these isoforms is shown in Figure 2. It can be seen that smooth and skeletal isoforms are of the same size, but differ by usage of exons 2a and 2b, and 9a and 9d. The two fibroblast isoforms are shorter due to their lack of exon 2, and both use the alternate exon 1b along with the smooth muscle-like exon 9a. The two differ internally by the use of either the muscle-like exon 6b or the non-muscle exon 6a. Comparison of the curves shows that the smooth and fibroblast isoforms are virtually identical but differ from the skeletal isoform. The parameters for the curve fits are shown in Table 2. These show that K_1 differs little between the different isoforms, showing that the different exon usages appear to have little effect upon the affinity of S1 for the actin−Tm complex. It also shows that there is little variance in the determined value of K_T between the isoforms, the significant difference between the curves being caused by a change in *n* from ~7 for skTm to 12−14 for the smooth and fibroblast Tms. It must, however, be pointed out that for the latter curves where the apparent cooperative unit is large the curves become less sigmoidal and the determined values for K_T and *n* are less well defined as can been seen in Figure 6C which shows simulations of curves generated with *n* varying from 1 to 14 with the other parameters set as for skTm.

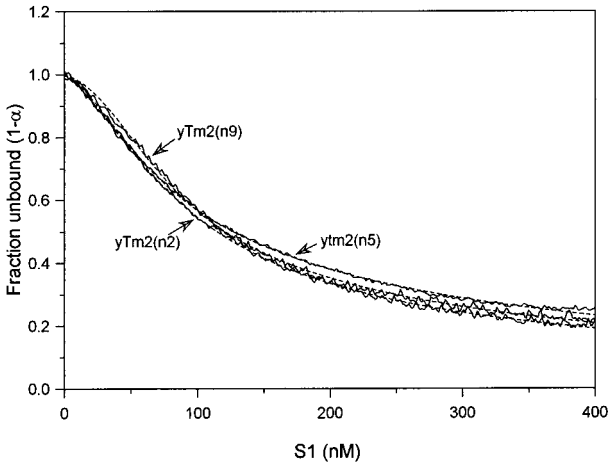

FIGURE 7: Myosin S1 binding curves under the same conditions described in the legend of Figure 6, including 50 nM actin in the presence of yTm2(*nX*) mutants (2 μM each) with curve fits superimposed with the values listed in Table 2.

Titration curves for the yTm2 constructs that have been produced are shown in Figure 7. These constructs are equivalent to those previously produced for yTm1 (*15*). As for Figure 6, the curves are shown with the curve fits superimposed, with the parameters for the fits shown in Table 2. The shapes of the curves differ from each other as seen previously for the similar yTm1 constructs. The curve fits show similar determined values for K_1 ($4.2-4.8 \times 10^4$ M^{-1}) and *n* (6−7) for all the yTm2 constructs. This shows that, as previously found for the yTm1 constructs, the differences between them are accounted for purely by changes in K_T.

DISCUSSION

The curve for S1 binding to the actin−Tm complex is represented in our model by four parameters, K_1, K_2, K_T, and *n*. K_2 is for the myosin isomerization from the A (attached) to R (rigor) states and is therefore a property of the actin−myosin interaction and hence invariant within the experiments here. It is set at the previously determined value of 200 (*30*). K_1 is for the binding of the weak A state and, therefore, governs the overall affinity (K_1K_2) of myosin for actin. The sigmoidicity of the curve is then defined by K_T [the closed (C) to open (M) equilibrium constant] which gives the occupancy of the two states and *n* (the apparent cooperative unit size) which is the apparent number of actin subunits that switch between each state.

Properties of yTm2 Constructs. The titrations for the yTm2 constructs show that they behave in a manner similar to that of the yTm1 constructs previously produced. They all bind to actin with a 50% saturation at ~0.5 μM, yet the three different constructs produce significantly different S1 binding curves. The parameters determined from the curve fits show that in each case the S1 affinity (K_1) and cooperative unit size *n* are similar. The variation between the curves is accounted for by changes in the value of K_T, the equilibrium constant for the C to M transition. The values show good agreement with those determined for the same N-terminal constructs made with yTm1 (see Table 2). Without data for

the K_T values of the native acetylated proteins, it is not possible to say which is the most native-like; however, the $n = 9$ constructs do produce a value of K_T (0.14 and 0.16) similar to those of the vertebrate Tms. It has previously been stated that recombinant skeletal Tm with the $n = 2$ (Ala-Ser) extension produces a native-like expressed skeletal Tm (*31*). This was assessed by Tm viscosity, affinity for actin, and ATPase level measurements. It will be of interest to contrast measurements of native proteins with measurements of these recombinant versions using the more sensitive regulatory assay system used here.

C to M (Closed−Open) Equilibrium (K_T) Values and Structural Data. All the vertebrate Tms when bound to actin show a similar equilibrium between the C and M states with K_T values of 0.1−0.15, in the absence of external influence (for example, in the presence of Tn or S1). However, 5a and 5b are both recombinant proteins and lack their native acetylation. As the N-terminal structure can influence K_T as shown by the N-terminal constructs of yTm1 and yTm2 discussed above, acetylation may likewise effect the determined K_T. This is a reflection of the fact that, as stated in our previous paper (*15*), the low value of K_T determined for the tropomyosins (mostly 0.1−0.15) shows there is a low energy barrier ($\Delta G°$) between the states. Hence, the equilibrium (K_T) is very sensitive to external influences such as sequence changes or possibly acetylation.

In general, the K_T values are in agreement with the structural data from cryo-em reconstructions of the same actin−Tm filaments (*9*). It was shown that native skTm ($\alpha\alpha$/$\alpha\beta$ mixture as used in this study), fibroblast 5a, and yTm1-(*n*5) (which was described as yeast N6 in that paper) all localized upon the inner domain, near junction inner and outer domains of actin (the C state). This is in agreement with our K_T values which place them predominantly in the C state [a K_T for yTm1(*n*5) of ≥1 gives as much as 50% C state]. The one disagreement is that smooth muscle Tm appears to be located structurally in the B state while our measurements show it to have a K_T similar to those of the other Tms. Pure skeletal $\alpha\alpha$ Tm (found in cardiac muscle) was also placed in the B state in the structural studies. This has not yet been studied by us and is of obvious interest for future work due to the significance of the cardiac system. However, so far there is no evidence of the B state from kinetic measurements (allowing for the detection limit of ∼20% occupancy) for any system containing Tm alone (*7*, *11*, *15*). Although only one of the Tms shows disparity with our measurements, this needs to be accounted for. The difference may be due in part to the methodology of data acquisition and helical reconstruction used to produce the structural images. There is always some selection of ordered filaments (those which produce good images) which are then averaged into a helical model to reconstruct the actin and Tm. This has the possibility of biasing the data toward "stable" forms and under estimating dynamic variations within the filament. These limitations may be overcome by using single-particle analysis of the em data sets which should allow a better resolution of the dynamics of this system.

Apparent Cooperative Unit Sizes (n). Generally, the cooperative unit sizes are larger than the structural unit size. All the vertebrate Tms have an apparent cooperative unit size of 12−14 with the notable exception of skTm. This is in agreement with previous measurements using fluorescently labeled skTm, smTm, and 5a (*11*). However, the native skeletal TmTn complex does have a similar cooperative unit size of ∼12 in the presence of Ca^{2+} (*12*, *13*) [in the absence of Ca^{2+}, the apparent cooperative unit size is dominated by the 1 per 7 pinning effect of TnI (*12*)]. The yeast Tms have an apparent cooperative unit size in the range of 6−7 and 8−9 for yTm2 and yTm1, respectively, also considerably larger than their structural unit size of 4 or 5. The considerable difference between the average cooperative unit size for the yeast and vertebrate Tms may indicate that there are innate flexibility differences between their sequences. Alternatively, there may be some relationship with the length of the Tms as the Tm−Tm junctions could provide a point of greater flexibility and hence greatly influence the apparent cooperativity. A more detailed study of the relationships of sequence and length with flexibility is needed to resolve which of the two effects is more significant.

The effect of varying *n* from 1 to 14 with the other parameters set as determined for skTm is shown in Figure 6C. As *n* becomes larger, the variation between the curves is reduced, meaning that at >10, *n* is no longer well defined. Previous studies also demonstrated that when K_T is large, *n* is no longer well defined (*15*). The interdependency of K_T and *n* means that for Tms with large values for either the exact values for both are not well defined by the titration method (which is currently the only method that can be used to measure K_T). However, a fluorescence probe on Tm can provide values of *n* independent of K_T (*11*), and these results are in agreement with those determined here.

Affinity of S1 and Tm for Actin. The data from the S1 titration experiments show a general 3-fold increase in K_1 caused by vertebrate Tms. This agrees with the complementary cosedimentation experiments in which the level of Tm binding to actin for skTm was measured, showing that the presence of S1 increases the affinity of skTm for actin by several orders of magnitude in agreement with many previous studies (*28*, *32*). The effect of S1 upon Tm affinity is expected to be thermodynamically coupled to the effect upon a single actin binding site, and since Tm spans 7 actin subunits, the increase should be approximately 3^7 (2187-fold) for skTm. It has been proposed these increases in affinity are caused by a conformational change in actin induced by the rigor binding of S1 in the presence of Tm, causing the formation of an open actin state with a higher affinity for both Tm and S1 (*28*, *29*, *33*). However, our measurements show that the increase in S1 affinity for actin produced by the vertebrate Tms appears to be unrelated to the regulation of S1 binding. Using yeast Tms, we show that the S1 affinity (K_1K_2) is the same as that for actin alone, and the complementary cosedimentation experiment with yTm1(*n*2) confirms there is little effect of S1 upon Tm affinity. Given our data for yTm2(*n*9) and skTm, they have very similar regulatory parameters in terms of both apparent cooperative unit size (7−8) and K_T (approximately 0.15), differing only in the value of K_1 which controls the affinity of S1 for actin. This indicates that the interaction of the two Tms with actin is similar as they both have a similar equilibrium between closed and open states and switch with the same unit size. An alternate explanation for these observations is a direct Tm−S1 interaction being responsible for the majority of the reciprocal effect upon the affinity of

S1 for actin. There is already some evidence for possible direct interaction between the myosin head and Tm from both cross-linking studies (*34*) and em structural data (*8*).

In combination, these results show that there appears to be little connection between Tm affinity for actin and its regulation of S1 binding. When the (*n*2) constructs of yTm1 and yTm2 and the vertebrate Tms are considered, all have similar values for K_T (0.1−0.36) but show a wide range of apparent cooperative unit sizes (7−14) which appear to be unrelated to their affinities. The most notable example is 5a and 5b which differ by an order of magnitude in their affinities for actin but show virtually identical regulatory parameters (the titration curves are indistinguishable and hence K_1, K_T, and n are the same).

This study shows the advantages of using yeast Tms to study the effect of varying Tm properties upon cooperativity parameters. Their smaller apparent cooperative unit size (especially compared to smooth muscle and fibroblast Tms) produces S1 binding curves that are more readily and accurately analyzed by our methods to allow relationships between structure and function to be determined. The absence of an increase in S1 affinity, while still showing regulation of the S1−actin interaction also allows regulation to be studied independently of such secondary effects.

REFERENCES

1. Lees-Miller, J. P., and Helfman, D. M. (1991) *BioEssays 13*, 429−437.
2. Lin, J. J., Warren, K. S., Wamboldt, D. D., Wang, T., and Lin, J. L. (1997) *Int. Rev. Cytol. 170*, 1−38.
3. Liu, H. P., and Bretscher, A. (1989) *Proc. Natl. Acad. Sci. U.S.A. 86*, 90−93.
4. Drees, B., Brown, C., Barrell, B. G., and Bretscher, A. (1995) *J. Cell Biol. 128*, 383−392.
5. Greene, L. E., and Eisenberg, E. (1980) *Proc. Natl. Acad. Sci. U.S.A. 77*, 2616−2620.
6. Lehrer, S. S., and Morris, E. P. (1982) *J. Biol. Chem. 257*, 8073−8080.
7. McKillop, D. F., and Geeves, M. A. (1993) *Biophys. J. 65*, 693−701.
8. Vibert, P., Craig, R., and Lehman, W. (1997) *J. Mol. Biol. 266*, 8−14.
9. Lehman, W., Hatch, V., Korman, V., Rosol, M., Thomas, L., Maytum, R., Geeves, M. A., Van Eyk, J. E., Tobacman, L. S., and Craig, R. (2000) *J. Mol. Biol. 302*, 593−606.
10. Hill, T. L., Eisenberg, E., and Greene, L. (1980) *Proc. Natl. Acad. Sci. U.S.A. 77*, 3186−3190.
11. Lehrer, S. S., Golitsina, N. L., and Geeves, M. A. (1997) *Biochemistry 36*, 13449−13454.
12. Maytum, R., Lehrer, S. S., and Geeves, M. A. (1999) *Biochemistry 38*, 1102−1110.
13. Geeves, M. A., and Lehrer, S. S. (1994) *Biophys. J. 67*, 273−282.
14. Schaertl, S., Lehrer, S. S., and Geeves, M. A. (1995) *Biochemistry 34*, 15890−15894.
15. Maytum, R., Geeves, M. A., and Konrad, M. (2000) *Biochemistry 39*, 11913−11920.
16. Novy, R. E., Liu, L. F., Lin, C. S., Helfman, D. M., and Lin, J. J. (1993) *Biochim. Biophys. Acta 1162*, 255−265.
17. Urbancikova, M., and Hitchcock-DeGregori, S. E. (1994) *J. Biol. Chem. 269*, 24310−24315.
18. Kluwe, L., Maeda, K., Miegel, A., Fujita-Becker, S., Maeda, Y., Talbo, G., Houthaeve, T., and Kellner, R. (1995) *J. Muscle Res. Cell Motil. 16*, 103−110.
19. Sambrook, J., Fritsh, E., and Maniatis, T. (1989) *Molecular Cloning A Laboratory Manual*, 2nd ed., Cold Spring Harbor Laboratory Press, Plainview, NY.
20. Konrad, M. (1993) *J. Biol. Chem. 268*, 11326−11334.
21. Weeds, A. G., and Taylor, R. S. (1975) *Nature 257*, 54−56.
22. Spudich, J. A., and Watt, S. (1971) *J. Biol. Chem. 246*, 4866−4871.
23. Criddle, A. H., Geeves, M. A., and Jeffries, T. (1985) *Biochem. J. 232*, 343−349.
24. Lehrer, S. S., and Stafford, W. F. d. (1991) *Biochemistry 30*, 5682−5688.
25. Laemmli, U. K. (1970) *Nature 227*, 680−685.
26. Pittenger, M. F., and Helfman, D. M. (1992) *J. Cell Biol. 118*, 841−858.
27. Hammell, R. L., and Hitchcock-DeGregori, S. E. (1997) *J. Biol. Chem. 272*, 22409−22416.
28. Moraczewska, J., Nicholson-Flynn, K., and Hitchcock-DeGregori, S. E. (1999) *Biochemistry 38*, 15885−15892.
29. Landis, C., Back, N., Homsher, E., and Tobacman, L. S. (1999) *J. Biol. Chem. 274*, 31279−31285.
30. McKillop, D. F., and Geeves, M. A. (1991) *Biochem. J. 279*, 711−718.
31. Monteiro, P. B., Lataro, R. C., Ferro, J. A., and Reinach, F. d. C. (1994) *J. Biol. Chem. 269*, 10461−10466.
32. Cassell, M., and Tobacman, L. S. (1996) *J. Biol. Chem. 271*, 12867−12872.
33. Moraczewska, J., and Hitchcock-DeGregori, S. E. (2000) *Biochemistry 39*, 6891−6897.
34. Golitsina, N. L., and Lehrer, S. S. (1999) *FEBS Lett. 463*, 146−150.

BI010072I